

The 3-dimensional distribution of quarks in momentum space

Alessandro Bacchetta,^{1,2,*} Filippo Delcarro,^{3,†} Cristian Pisano,^{4,5,‡} and Marco Radici^{2,§}

¹*Dipartimento di Fisica Nucleare e Teorica, Università di Pavia*

²*INFN Sezione di Pavia, via Bassi 6, I-27100 Pavia, Italy*

³*Jefferson Lab, 12000 Jefferson Avenue, Newport News, Virginia 23606, USA*

⁴*Dipartimento di Fisica, Università di Cagliari, Cittadella Universitaria, I-09042 Monserrato (CA), Italy*

⁵*INFN Sezione di Cagliari, Cittadella Universitaria, I-09042 Monserrato (CA), Italy*

We present the distribution of unpolarized quarks in a transversely polarized proton in three-dimensional momentum space. Our results are entirely based on transverse-momentum-dependent parton distributions (TMDs) extracted in a consistent way from experimental measurements.

The antipode of taking a picture of a black hole is taking a picture of the inside of a proton, unlocking its internal constituents, confined in the most common element of the visible universe by the strong forces of Quantum Chromodynamics (QCD). Using data from the scattering of a hard virtual photon off a proton, we map the density of quarks in three dimensions, i.e., as a function of their longitudinal momentum (along the photon's direction) and their transverse momentum (orthogonal to the photon). If the proton is unpolarized, the distribution is cylindrically symmetric: we determine it using recent results from our group [12]. If the proton is polarized in the transverse plane, the distributions of up and down quarks turn out to be distorted in opposite directions. This distortion, known as Sivers effect [39], is related to quark orbital angular momentum. We determine its details with the same formalism used for the unpolarized distribution. In this way, we obtain a consistent picture of the full 3-dimensional momentum distribution of quarks in a transversely polarized proton. Our study constitutes a benchmark for future determinations of multi-dimensional quark distributions, one of the main goals of existing and planned experimental facilities [1, 7, 25].

We consider a frame where the proton has momentum P with space component in the $+z$ direction, is polarized in the $+y$ direction, and is probed by a spacelike virtual photon with momentum q (with $Q^2 = -q^2$) in the $-z$ direction. We define the xy plane as transverse and we denote it with the subscript T . We consider the light-cone $+$ direction $(t+z)/\sqrt{2}$ and we define it as longitudinal. If Q^2 is much larger than the proton's mass M^2 , the proton's momentum is approximately longitudinal (P^+ is the dominant component).

Our goal is to reconstruct the distribution of unpolarized quarks inside the nucleon as a function of three components of their momentum. In the frame we are considering, the distribution of a quark with flavor a in a transversely polarized nucleon N^\uparrow can be written in terms of

two Transverse Momentum Distributions (TMDs) as [10]

$$\rho_{N^\uparrow}^a(x, k_x, k_y; Q^2) = f_1^a(x, k_T^2; Q^2) - f_{1T}^{\perp a}(x, k_T^2; Q^2) \frac{k_x}{M}, \quad (1)$$

where f_1^a is the unpolarized TMD and $f_{1T}^{\perp a}$ is the Sivers TMD [39], k is the momentum of the quark, k_T its transverse component, and $x = k^+/P^+$ is its longitudinal momentum fraction. Q^2 plays the role of a resolution scale.

Recent extractions of f_1 have been published in Refs. [12, 13, 15, 38]. Several parametrizations of f_{1T}^{\perp} have been released up to now [5, 6, 9, 18, 22, 26, 40?, 41]. In this work, we start from a recent determination of f_1 by our group [12] and we extract f_{1T}^{\perp} using the same formalism. Thus, for the first time we consistently reconstruct the full 3-dimensional quark density of Eq. (1).

Both unpolarized and Sivers TMDs appear in the cross section of polarized Semi-Inclusive Deep-Inelastic Scattering (SIDIS), i.e., the process $\ell(l) + N(P) \rightarrow \ell(l') + h(P_h) + X$, where a lepton ℓ with momentum l scatters off a nucleon target N with mass M and momentum P . In the final state, the scattered lepton with momentum $l' = l - q$ is detected, together with a hadron h with momentum P_h and transverse momentum P_{hT} . We define the usual SIDIS variables $x_{Bj} = \frac{Q^2}{2P \cdot q}$, $z = \frac{P \cdot P_h}{P \cdot q}$. In this study, we neglect power corrections of order M^2/Q^2 and P_{hT}^2/Q^2 , which allow us also to identify $x_{Bj} = x$.

The SIDIS cross section can be written in terms of structure functions [11] that can be measured experimentally. Factorization theorems make it possible to write the structure functions at small transverse momentum ($P_{hT}^2 \ll Q^2$) in terms of TMDs and to derive evolution equations that predict how TMDs change as functions of two scales μ^2 and ζ [23]. These two scales are usually chosen to be equal to the virtual photon mass Q^2 .

The unpolarized TMD f_1 enters the structure function $F_{UU,T}$. The Sivers TMD f_{1T}^{\perp} enters the structure function $F_{UT,T}^{\sin(\phi_h - \phi_S)}$, which occurs in the polarized part of the cross section weighted by $\sin(\phi_h - \phi_S)$, where ϕ_h and ϕ_S indicate the azimuthal orientations of \mathbf{P}_{hT} and the target polarization \mathbf{S}_T in the transverse plane, respectively. Both structure functions can be defined as convolutions of TMDs upon quark transverse momenta. Their Fourier

* alessandro.bacchetta@unipv.it

† delcarro@jlab.org

‡ cristian.pisano@unica.it

§ marco.radici@pv.infn.it

transform can be written more conveniently as a product of the Fourier transforms of TMDs, i.e.,¹

$$\tilde{F}_{UU,T}(x, z, b_T^2, Q^2) = \sum_a e_a^2 x \tilde{f}_1^a(x, b_T^2; Q^2) \tilde{D}_1^{a \rightarrow h}(z, b_T^2; Q^2), \quad (2)$$

$$\tilde{F}_{UT,T}^{\sin(\phi_h - \phi_s)}(x, z, b_T^2, Q^2) = -M \sum_a e_a^2 x \tilde{f}_{1T}^{\perp(1)a}(x, b_T^2; Q^2) \tilde{D}_1^{a \rightarrow h}(z, b_T^2; Q^2), \quad (3)$$

where we introduced the first derivative of the Siverson function in Fourier space [17]:

$$\tilde{f}_{1T}^{\perp(1)a}(x, b_T^2; Q^2) = -\frac{2}{M^2} \partial_{b_T^2} \tilde{f}_{1T}^{\perp a}(x, b_T^2; Q^2). \quad (4)$$

The above equation, evaluated at $b_T = 0$, gives the first transverse moment of the Siverson function

$$f_{1T}^{\perp(1)a}(x; Q^2) = \tilde{f}_{1T}^{\perp(1)a}(x, 0; Q^2), \quad (5)$$

which is an x -dependent function and corresponds to the so-called Qiu-Sterman function [16, 35].

Apart from the unpolarized TMD f_1 and the Siverson TMD f_{1T}^{\perp} , the above equations contain also the Fourier transform of the unpolarized transverse-momentum-dependent fragmentation function D_1 , another essential ingredient for the extraction of the Siverson function.

In this work, we take the unpolarized functions f_1 and D_1 from our own extraction of Ref. [12], which we denote as Pavia17. We extract the Siverson function using the same approach, based on the work of Collins, Soper, Sterman (CSS) [23, 24]. The analysis is done at the next-to-leading-logarithmic (NLL) accuracy, as defined in detail in [13].² We avoid diverging perturbative contributions using the so-called b^* prescription and introducing a universal nonperturbative term in the TMD evolution, common to the unpolarized and Siverson TMDs. At variance with the standard CSS approach, we also modify the high-transverse-momentum behavior of TMDs through the so-called b_{min} prescription.

We write the Siverson function at the initial scale ($Q_0 = 1$ GeV) as a product of a suitably normalized k_T -dependent function and the first transverse moment, $f_{1T}^{\perp(1)}$. The function reads

$$f_{1T}^{\perp a}(x, k_T^2; Q_0^2) = f_{1T}^{\perp(1)a}(x; Q_0^2) f_{1TNP}^{\perp}(x, k_T^2). \quad (6)$$

The nonperturbative term f_{1TNP}^{\perp} is given by

$$f_{1TNP}^{\perp}(x, k_T^2) = \frac{(1 + \lambda_S k_T^2) e^{-k_T^2/M_1^2}}{K\pi (M_1^2 + \lambda_S M_1^4)} f_{1NP}(x, k_T^2), \quad (7)$$

where the f_{1NP} is consistently taken from the Pavia17 extraction. The M_1, λ_S are free parameters, and K is the normalization factor. The first transverse moment is parametrized as

$$f_{1T}^{\perp(1)a}(x; Q_0^2) = \frac{N_{Siv}^a}{G_{max}^a} x^{\alpha_a} (1-x)^{\beta_a} \times [1 + A_a T_1(x) + B_a T_2(x)] f_1(x; Q_0^2), \quad (8)$$

where $T_n(x)$ are Chebyshev polynomials of order n , and f_1 are collinear parton densities consistently taken from the same set used in the Pavia17 fit [28]. The flavor-dependent factor G_{max}^a is introduced to guarantee the positivity bound of the Siverson function of Eq. (6) [8]. The free parameters N_{Siv} (varying only between -1 and 1), α, β, A, B are different for up, down, and sea quarks. The total number of free parameters is 17.

To compute the Siverson function at a generic scale Q^2 , we apply TMD evolution at NLL. This is more conveniently written in b_T space and leads to

$$\tilde{f}_{1T}^{\perp(1)a}(x, b_T^2; Q^2) = e^{S(\mu_b^2, Q^2)} e^{g_K(b_T) \ln(Q^2/Q_0^2)} \times f_{1T}^{\perp(1)a}(x; \mu_b^2) \tilde{f}_{1TNP}^{\perp(1)a}(x, b_T^2), \quad (9)$$

where μ_b is a scale proportional to $1/b_T$. With our prescriptions, we always have $Q_0 \leq \mu_b \leq Q$. At the initial scale Q_0 , the exponentials reduce to unity and the above equation indeed corresponds to the derivative of the Fourier transform of Eq. (6). For the transverse moment $f_{1T}^{\perp(1)}$, we apply the same evolution as the collinear PDF f_1 using the HOPPET code [37]. This is an approximation of the full evolution [31], but we checked that modifying this part of the evolution does not lead to significant changes. Much more relevant for TMD evolution are the Sudakov form factor S and the function $g_K(b_T)$: they are present also in the unpolarized TMD function f_1 and are again taken from the Pavia17 fit. Without this information, it would not be possible to reliably calculate the Siverson function at the experimental scales.

We fix the free parameters of our functional form by fitting experimental data for single transverse-spin asymmetries [10]

$$A_{UT}^{\sin(\phi_h - \phi_s)}(x, z, \mathbf{P}_{hT}^2, Q^2) \approx \frac{F_{UT,T}^{\sin(\phi_h - \phi_s)}}{F_{UU,T}}. \quad (10)$$

An accurate extraction requires the inclusion of asymmetry measurements taken by different experimental collaborations, covering different ranges of kinematic variables, using different type of targets and final-state hadrons. In our fit we include measurements published by the HERMES [3], COMPASS [2, 4] and JLab collaborations [34]. Usually, the asymmetries are presented as projections of the same dataset in x, z , and P_{hT} . To avoid fully correlated measurements, we fit only the x projections, since we are mainly interested in the x -dependence of the Siverson function. We select data by applying the same criteria used for the unpolarized TMD fit, i.e., $Q^2 > 1.4$

¹ More details are given in the supplemental material

² At this accuracy, the hard functions and the matching coefficients can be neglected.

GeV^2 , $0.20 < z < 0.74$ and $P_{hT} < \min[0.2Q, 0.7Qz] + 0.5$ GeV. After these kinematic cuts, we have a total of 118 data points: 30 from HERMES, 82 from COMPASS (32 from the 2009 analysis, and 50 from the 2017 analysis), and 6 from JLab.

Similarly to our previous Pavia17 extraction and to other studies of parton densities [14, 27, 36], we perform the fit using the bootstrap method. The method consists in creating \mathcal{M} different replicas of the original data by randomly shifting them with a Gaussian noise with the same variance as the experimental measurement. Each replica represents the possible outcome of an independent measurement. We then fit each replica separately and we obtain a vector of \mathcal{M} results for each free parameter. The number \mathcal{M} is fixed by accurately reproducing the mean and standard deviation of the original data points. In our case, it turns out $\mathcal{M} = 200$, which is also consistent with our Pavia17 fit [12].

The maximal information about our results is given by the full ensemble of 200 replicas, combined with the corresponding unpolarized TMD replicas. To report our results in a concise way, we adopt the following choice: for any result (χ^2 values, parameter values, resulting distribution functions) we quote intervals containing 68% of the replicas, obtained by including the upper 16% and lower 16% values. These intervals correspond to the 1σ confidence level only if the observable's values follow a Gaussian distribution, which is not true in general. When it is not possible to draw uncertainty bands, we report the results obtained using replica 105, which we consider one of the most representative replicas.

We obtain an excellent agreement between the experimental measurements and our theoretical prediction, with an overall value of $\chi^2/\text{d.o.f.} = 1.1 \pm 0.1$ (total $\chi^2 = 110 \pm 11$). Our parametrization is able to describe very well the COMPASS 2009 data set (32 points with $\chi^2 = 30 \pm 5$), the COMPASS 2017 data set (50 points with $\chi^2 = 31 \pm 5$), and the JLab data set (6 points with $\chi^2 = 5 \pm 2$). The agreement with the HERMES data set is worse (30 points with $\chi^2 = 48 \pm 7$). We checked that the largest contribution to the χ^2 comes from the subset of data with K^- in the final state. Our predictions well describe also the z and P_{hT} distributions, even if those projections of the data were not included in the fit. (More information about the fit procedure, the best-fit parameters and the agreement with data can be found in the Supplemental Material.)

In Fig. 1, we show the first transverse moment $xf_{1T}^{\perp(1)}$ (Eq. (5)), multiplied by x as a function of x at $Q_0^2 = 2$ GeV² for the up (upper panel) and down quark (lower panel). We compare our results (solid band) with other parametrizations available in the literature [9, 18, 26]

(hatched bands, as indicated in the figure). In agreement with previous studies, the distribution for the up quark is negative, while for the down quark is positive and both have a similar magnitude. The Sivvers function for sea quarks is very small but not compatible with zero.

In general, the result of a fit is biased whenever a spe-

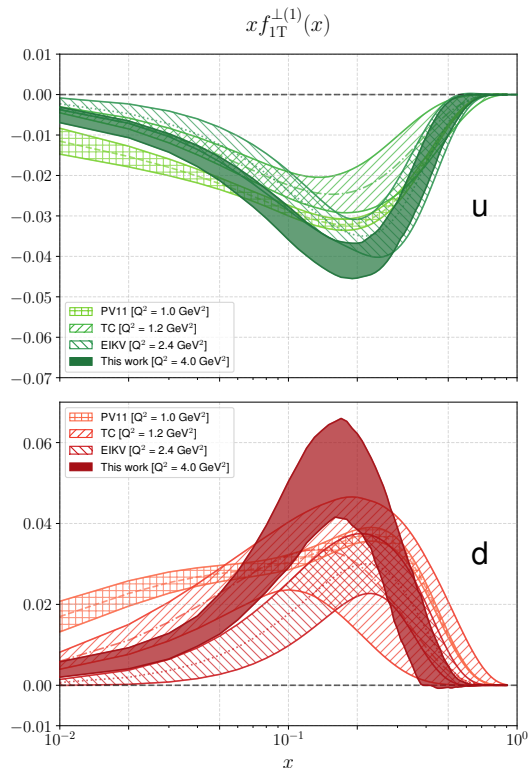


FIG. 1. The first transverse moment $xf_{1T}^{\perp(1)}$ of the Sivvers TMD as a function of x for the up (upper panel) and down quark (lower panel). Solid band for the 68% uncertainty band of this fit at $Q_0^2 = 2$ GeV². Hatched bands from other extractions at different Q_0^2 as indicated in the figure.

cific fitting functional form is chosen at the initial scale. In our case, we tried to reduce this bias by adopting a flexible functional form, as it is evident particularly in Eq. (8). Nevertheless, we stress that our extraction is still affected by this bias and extrapolations outside the range where data exist ($0.01 \lesssim x \lesssim 0.3$) should be taken with due care. At variance with other studies, in the denominator of the asymmetry in Eq. (10) we are using unpolarized TMDs that were extracted from data in our previous Pavia17 fit, with their own uncertainties. Therefore, our uncertainty bands in Fig. 1 represent the most realistic estimate that we can currently make on the statistical error of the Sivvers function.

In Fig. 2, we show the density distribution $\rho_{p\uparrow}^a$ of unpolarized quarks in a transversely polarized proton defined

in Eq. (1), at $x = 0.1$ (upper panels) and $x = 0.01$ (lower panels) and at the scale $Q^2 = 4$ GeV². The proton is

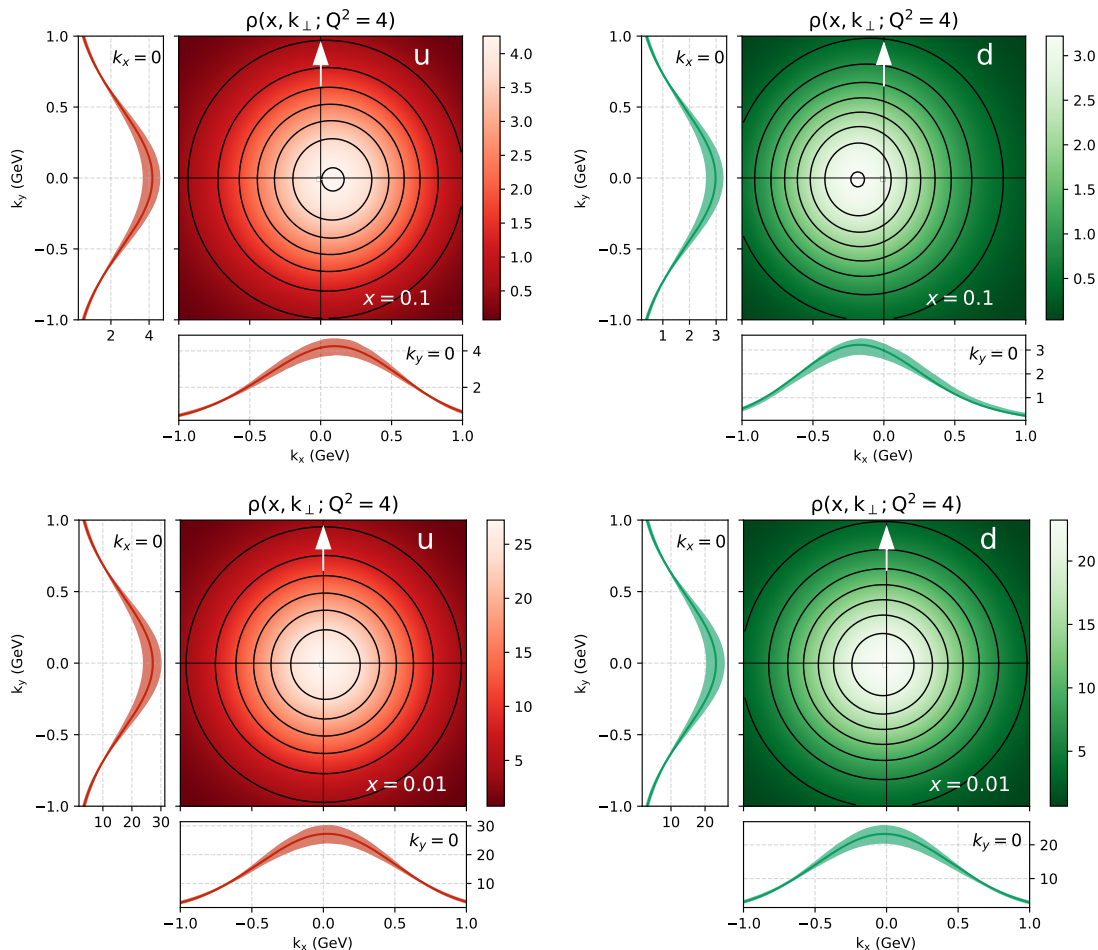


FIG. 2. The density distribution of unpolarized quarks in a proton transversely polarized along the $+y$ direction and moving towards the reader, as a function of (k_x, k_y) at $Q^2 = 4 \text{ GeV}^2$. Left panels for the up quark, right panels for the down quark. Upper panels for results at $x = 0.1$, lower panels at $x = 0.01$. For each panel, lower ancillary plots represent the 68% uncertainty band of the distribution at $k_y = 0$ (where the effect of the distortion due to the Sivers function is maximal) while left ancillary plots at $k_x = 0$ (where the distribution is the same as for an unpolarized proton). Results in the contour plots and the solid lines in the projections correspond to replica 105. The bands in the projections contain 68% of the results obtained with 200 replicas of the fit.

moving towards the reader and is polarized along the $+y$ direction. Since the up Sivers function is negative, the induced distortion is positive along the $+x$ direction for the up quark (left panels), and opposite for the down quark (right panels).

At $x = 0.1$ the distortion due to the Sivers effect is evident, since we are close to the maximum value of the function shown in Fig. 1. The distortion is opposite for up and down quarks, reflecting the opposite sign of the Sivers function. It is more pronounced for down quarks, because the Sivers function is larger and at the same time the unpolarized TMD is smaller. At lower values of x , the distortion disappears. These plots suggest that a virtual photon hitting a transversely polarized proton effectively “sees” more up quarks to its right and more down quarks to its left in momentum space. The peak positions are approximately $(k_x)_{\text{max}} \approx 0.1 \text{ GeV}$ for up quarks and -0.15

GeV for down quarks. To have a feeling of the order of magnitude of this distortion, we can estimate the expression $e_q/(k_x)_{\text{max}} \approx 2 \times 10^{-34} C \times m \approx 0.6 \times 10^{-4}$ debye, which is about 3×10^{-5} times the electric dipole of a water molecule.

The existence of this distortion requires two ingredients. First of all, the wavefunction describing quarks inside the proton must have a component with nonvanishing angular momentum. Secondly, effects due to final state interactions should be present [19], which in Feynman gauge can be described as the exchange of Coulomb gluons between the quark and the rest of the proton [30]. In simplified models [33], it is possible to separate these two ingredients and obtain an estimate of the angular momentum carried by each quark [21]. It turns out that up quarks give almost 50% contribution to the proton’s spin, while all other quarks and antiquarks give less than

10% [9]. We will leave this model-dependent study to a future publication. A model-independent estimate of quark angular momentum requires the determination of parton distributions that depend simultaneously on momentum and position [29, 32]. Nevertheless, the study of TMDs, and of the Sivers function in particular, can provide important constraints on models of the nucleon [20] and test lattice QCD computations [42].

In the near future, more data are expected from experiments at Jefferson Laboratory and CERN. Pioneering measurements in Drell-Yan processes have been already reported, but they are not included in the present analysis because of their relatively large uncertainties. In the longer term, the recently approved Electron Ion Collider project [1] will provide a large amount of data in different kinematic regions compared to present experiments.

With this abundance of data, we will be able to reduce the error bands, extend the range of validity of the extractions to lower and higher values of x , and obtain a much more detailed knowledge of the 3-dimensional distribution of partons in momentum space.

ACKNOWLEDGMENTS

This work is supported by the European Research Council (ERC) under the European Union’s Horizon 2020 research and innovation program (grant agreement No. 647981, 3DSPIN). This material is based upon work supported by the U.S. Department of Energy, Office of Science, Office of Nuclear Physics under contract DE-AC05-06OR23177.

-
- [1] A. Accardi et al. Electron Ion Collider: The Next QCD Frontier. *Eur. Phys. J.*, A52(9):268, 2016. doi:10.1140/epja/i2016-16268-9.
- [2] C Adolph et al. Sivers asymmetry extracted in SIDIS at the hard scales of the Drell-Yan process at COMPASS. *Phys. Lett.*, B770:138–145, 2017. doi:10.1016/j.physletb.2017.04.042.
- [3] A. Airapetian et al. Observation of the Naive-T-odd Sivers Effect in Deep-Inelastic Scattering. *Phys. Rev. Lett.*, 103:152002, 2009. doi:10.1103/PhysRevLett.103.152002.
- [4] M. Alekseev et al. Collins and Sivers asymmetries for pions and kaons in muon-deuteron DIS. *Phys. Lett.*, B673:127–135, 2009. doi:10.1016/j.physletb.2009.01.060.
- [5] M. Anselmino, M. Boglione, U. D’Alesio, A. Kotzinian, F. Murgia, and A. Prokudin. Extracting the Sivers function from polarized SIDIS data and making predictions. *Phys. Rev.*, D72:094007, 2005. doi:10.1103/PhysRevD.72.094007, 10.1103/PhysRevD.72.099903. [Erratum: *Phys. Rev.D72,099903(2005)*].
- [6] M. Anselmino, M. Boglione, U. D’Alesio, A. Kotzinian, S. Melis, F. Murgia, A. Prokudin, and C. Turk. Sivers Effect for Pion and Kaon Production in Semi-Inclusive Deep Inelastic Scattering. *Eur. Phys. J.*, A39:89–100, 2009. doi:10.1140/epja/i2008-10697-y.
- [7] Elke-Caroline Aschenauer et al. The RHIC Cold QCD Plan for 2017 to 2023: A Portal to the EIC. 2016.
- [8] A. Bacchetta, Mariaelena Boglione, A. Henneman, and P. J. Mulders. Bounds on transverse momentum dependent distribution and fragmentation functions. *Phys. Rev. Lett.*, 85:712–715, 2000. doi:10.1103/PhysRevLett.85.712.
- [9] Alessandro Bacchetta and Marco Radici. Constraining quark angular momentum through semi-inclusive measurements. *Phys. Rev. Lett.*, 107:212001, 2011. doi:10.1103/PhysRevLett.107.212001.
- [10] Alessandro Bacchetta, Umberto D’Alesio, Markus Diehl, and C. Andy Miller. Single-spin asymmetries: The Trento conventions. *Phys. Rev.*, D70:117504, 2004. doi:10.1103/PhysRevD.70.117504.
- [11] Alessandro Bacchetta, Markus Diehl, Klaus Goeke, Andreas Metz, Piet J. Mulders, and Marc Schlegel. Semi-inclusive deep inelastic scattering at small transverse momentum. *JHEP*, 02:093, 2007. doi:10.1088/1126-6708/2007/02/093.
- [12] Alessandro Bacchetta, Filippo Delcarro, Cristian Pisano, Marco Radici, and Andrea Signori. Extraction of partonic transverse momentum distributions from semi-inclusive deep-inelastic scattering, Drell-Yan and Z-boson production. *JHEP*, 06:081, 2017. doi:10.1007/JHEP06(2017)081, 10.1007/JHEP06(2019)051. [Erratum: *JHEP06,051(2019)*].
- [13] Alessandro Bacchetta, Valerio Bertone, Chiara Bisolotti, Giuseppe Bozzi, Filippo Delcarro, Fulvio Piacenza, and Marco Radici. Transverse-momentum-dependent parton distributions up to N^3 LL from Drell-Yan data. 2019.
- [14] Richard D. Ball, Luigi Del Debbio, Stefano Forte, Alberto Guffanti, Jose I. Latorre, Juan Rojo, and Maria Ubiali. A first unbiased global NLO determination of parton distributions and their uncertainties. *Nucl. Phys.*, B838:136–206, 2010. doi:10.1016/j.nuclphysb.2010.05.008.
- [15] Valerio Bertone, Ignazio Scimemi, and Alexey Vladimirov. Extraction of unpolarized quark transverse momentum dependent parton distributions from Drell-Yan/Z-boson production. *JHEP*, 06:028, 2019. doi:10.1007/JHEP06(2019)028.
- [16] Daniel Boer, P. J. Mulders, and F. Pijlman. Universality of T odd effects in single spin and azimuthal asymmetries. *Nucl. Phys.*, B667:201–241, 2003. doi:10.1016/S0550-3213(03)00527-3.
- [17] Daniel Boer, Leonard Gamberg, Bernhard Musch, and Alexei Prokudin. Bessel-Weighted Asymmetries in Semi Inclusive Deep Inelastic Scattering. *JHEP*, 10:021, 2011. doi:10.1007/JHEP10(2011)021.
- [18] M. Boglione, U. D’Alesio, C. Flore, and J. O. Gonzalez-Hernandez. Assessing signals of TMD physics in SIDIS azimuthal asymmetries and in the extraction of the Sivers function. *JHEP*, 07:148, 2018. doi:10.1007/JHEP07(2018)148.
- [19] Stanley J. Brodsky, Dae Sung Hwang, and Ivan Schmidt. Final state interactions and single spin asymmetries in

- semiinclusive deep inelastic scattering. *Phys. Lett.*, B530: 99–107, 2002. doi:10.1016/S0370-2693(02)01320-5.
- [20] M. Burkardt and B. Pasquini. Modelling the nucleon structure. *Eur. Phys. J.*, A52(6):161, 2016. doi:10.1140/epja/i2016-16161-7.
- [21] Matthias Burkardt. Impact parameter dependent parton distributions and transverse single spin asymmetries. *Phys. Rev.*, D66:114005, 2002. doi:10.1103/PhysRevD.66.114005.
- [22] J. C. Collins, A. V. Efremov, K. Goeke, S. Menzel, A. Metz, and P. Schweitzer. Sivers effect in semi-inclusive deeply inelastic scattering. *Phys. Rev.*, D73:014021, 2006. doi:10.1103/PhysRevD.73.014021.
- [23] John Collins. Foundations of perturbative QCD. *Camb. Monogr. Part. Phys. Nucl. Phys. Cosmol.*, 32:1–624, 2011.
- [24] John C. Collins, Davison E. Soper, and George F. Sterman. Transverse Momentum Distribution in Drell-Yan Pair and W and Z Boson Production. *Nucl. Phys.*, B250: 199–224, 1985. doi:10.1016/0550-3213(85)90479-1.
- [25] Jozef Dudek et al. Physics Opportunities with the 12 GeV Upgrade at Jefferson Lab. *Eur. Phys. J.*, A48:187, 2012. doi:10.1140/epja/i2012-12187-1.
- [26] Miguel G. Echevarria, Ahmad Idilbi, Zhong-Bo Kang, and Ivan Vitev. QCD Evolution of the Sivers Asymmetry. *Phys. Rev.*, D89:074013, 2014. doi:10.1103/PhysRevD.89.074013.
- [27] Stefano Forte, Lluís Garrido, Jose I. Latorre, and Andrea Piccione. Neural network parametrization of deep inelastic structure functions. *JHEP*, 05:062, 2002. doi:10.1088/1126-6708/2002/05/062.
- [28] M. Gluck, P. Jimenez-Delgado, and E. Reya. Dynamical parton distributions of the nucleon and very small- x physics. *Eur. Phys. J.*, C53:355–366, 2008. doi:10.1140/epjc/s10052-007-0462-9.
- [29] Xiang-Dong Ji. Gauge-Invariant Decomposition of Nucleon Spin. *Phys. Rev. Lett.*, 78:610–613, 1997. doi:10.1103/PhysRevLett.78.610.
- [30] Xiang-dong Ji and Feng Yuan. Parton distributions in light cone gauge: Where are the final state interactions? *Phys. Lett.*, B543:66–72, 2002. doi:10.1016/S0370-2693(02)02384-5.
- [31] Zhong-Bo Kang and Jian-Wei Qiu. QCD evolution of naive-time-reversal-odd parton distribution functions. *Phys. Lett. B*, 713:273–276, 2012. doi:10.1016/j.physletb.2012.06.021.
- [32] Cedric Lorce, Barbara Pasquini, Xiaonu Xiong, and Feng Yuan. The quark orbital angular momentum from Wigner distributions and light-cone wave functions. *Phys. Rev.*, D85:114006, 2012. doi:10.1103/PhysRevD.85.114006.
- [33] Barbara Pasquini, Simone Rodini, and Alessandro Bacchetta. Revisiting model relations between T-odd transverse-momentum dependent parton distributions and generalized parton distributions. *Phys. Rev.*, D100(5):054039, 2019. doi:10.1103/PhysRevD.100.054039.
- [34] X. Qian et al. Single Spin Asymmetries in Charged Pion Production from Semi-Inclusive Deep Inelastic Scattering on a Transversely Polarized ^3He Target. *Phys. Rev. Lett.*, 107:072003, 2011. doi:10.1103/PhysRevLett.107.072003.
- [35] Jian-wei Qiu and George F. Sterman. Single transverse spin asymmetries in hadronic pion production. *Phys. Rev.*, D59:014004, 1999. doi:10.1103/PhysRevD.59.014004.
- [36] Marco Radici, A. Courtoy, Alessandro Bacchetta, and Marco Guagnelli. Improved extraction of valence transversity distributions from inclusive di-hadron production. *JHEP*, 05:123, 2015. doi:10.1007/JHEP05(2015)123.
- [37] Gavin P. Salam and Juan Rojo. A Higher Order Perturbative Parton Evolution Toolkit (HOPPET). *Comput. Phys. Commun.*, 180:120–156, 2009. doi:10.1016/j.cpc.2008.08.010.
- [38] Ignazio Scimemi and Alexey Vladimirov. Non-perturbative structure of semi-inclusive deep-inelastic and Drell-Yan scattering at small transverse momentum. 2019.
- [39] Dennis W. Sivers. Single Spin Production Asymmetries from the Hard Scattering of Point-Like Constituents. *Phys. Rev.*, D41:83, 1990. doi:10.1103/PhysRevD.41.83.
- [40] Peng Sun and Feng Yuan. Transverse momentum dependent evolution: Matching semi-inclusive deep inelastic scattering processes to Drell-Yan and W/Z boson production. *Phys. Rev. D*, 88(11):114012, 2013. doi:10.1103/PhysRevD.88.114012.
- [41] Werner Vogelsang and Feng Yuan. Single-transverse spin asymmetries: From DIS to hadronic collisions. *Phys. Rev.*, D72:054028, 2005. doi:10.1103/PhysRevD.72.054028.
- [42] Boram Yoon, Michael Engelhardt, Rajan Gupta, Tanmoy Bhattacharya, Jeremy R. Green, Bernhard U. Musch, John W. Negele, Andrew V. Pochinsky, Andreas Schäfer, and Sergey N. Syritsyn. Nucleon Transverse Momentum-dependent Parton Distributions in Lattice QCD: Renormalization Patterns and Discretization Effects. *Phys. Rev.*, D96(9):094508, 2017. doi:10.1103/PhysRevD.96.094508.

Appendix A: Supplemental material

1. Fourier transforms of structure functions

The structure functions of Eqs. (2) and (3) can be written more explicitly as [17]

$$\begin{aligned} F_{UU,T}(x, z, \mathbf{P}_{hT}^2, Q^2) &= \frac{1}{2\pi} \int_0^\infty db_T b_T J_0(b_T |\mathbf{P}_{hT}|/z) \tilde{F}_{UU,T}(x, z, b_T^2, Q^2) \\ &= \frac{1}{2\pi} \sum_a e_a^2 x \int_0^\infty db_T b_T J_0(b_T |\mathbf{P}_{hT}|/z) \tilde{f}_1^a(x, b_T^2; Q^2) \tilde{D}_1^{a \rightarrow h}(z, b_T^2; Q^2), \end{aligned} \quad (\text{A1})$$

$$\begin{aligned} F_{UT,T}^{\sin(\phi_h - \phi_s)}(x, z, \mathbf{P}_{hT}^2, Q^2) &= \frac{1}{2\pi} \int_0^\infty db_T b_T^2 J_1(b_T |\mathbf{P}_{hT}|/z) \tilde{F}_{UT,T}^{\sin(\phi_h - \phi_s)}(x, z, b_T^2, Q^2) \\ &= -\frac{M}{2\pi} \sum_a e_a^2 x \int_0^\infty db_T b_T^2 J_1(b_T |\mathbf{P}_{hT}|/z) \tilde{f}_{1T}^{\perp(1)a}(x, b_T; Q^2) \tilde{D}_1^{a \rightarrow h}(z, b_T^2; Q^2). \end{aligned} \quad (\text{A2})$$

The Fourier transforms of the TMDs are defined as

$$\tilde{f}_1^a(x, b_T^2; Q^2) = \int d^2 \mathbf{k}_T e^{ib_T \cdot \mathbf{k}_T} f_1^a(x, k_T^2; Q^2) = \pi \int_0^\infty d|\mathbf{k}_T|^2 J_0(b_T |\mathbf{k}_T|) f_1^a(x, k_T^2; Q^2) \quad (\text{A3})$$

$$\tilde{f}_{1T}^{\perp(1)a}(x, b_T^2; Q^2) = \int d^2 \mathbf{k}_T e^{ib_T \cdot \mathbf{k}_T} \frac{|\mathbf{k}_T|^2}{2M^2} f_1^a(x, k_T^2; Q^2) = \frac{\pi}{M^2} \int_0^\infty d|\mathbf{k}_T|^2 \frac{|\mathbf{k}_T|}{b_T} J_1(b_T |\mathbf{k}_T|) f_{1T}^{\perp a}(x, k_T^2; Q^2). \quad (\text{A4})$$

Note that there is a factor 2π difference compared to the definition in the Pavia17 extraction [12], which has been taken into account in the rest of the article.

2. Details about the fit

We denote the replicated measurements as A_r^{Siv} , with the r index running from 1 to \mathcal{M} . Once replicas are generated, a minimization procedure is applied to each replica separately to search for the parameter values, $\{p_{r0}\}$, that minimize the error function

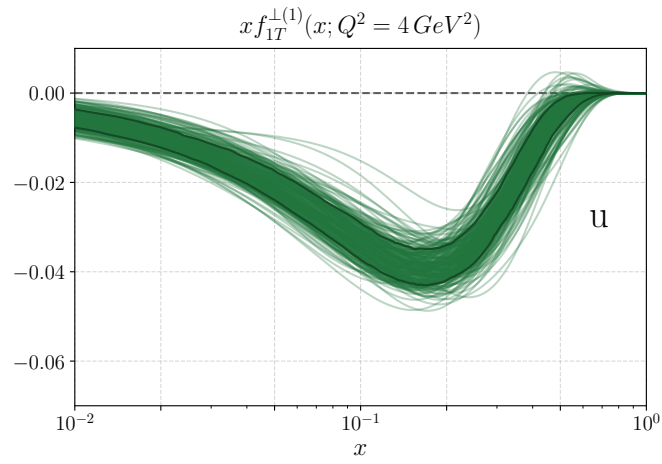
$$E_r^2(\{p_r\}) = \sum_i \frac{\left(A_r^{\text{Siv}} - A_{\text{th}}^{\text{Siv}}(\{p_r\}) \right)_i^2}{(\Delta A_{\text{stat}}^{\text{Siv}})_i^2 + (\Delta A_{\text{sys}}^{\text{Siv}})_i^2 + (\Delta A_{\text{th}}^{\text{Siv}})_i^2}. \quad (\text{A5})$$

The terms in the denominator are the statistical and systematic experimental errors, assumed to be completely uncorrelated, and the theoretical error due to the uncertainty in the unpolarized TMDs. For each replica separately, we identify the minimum and the corresponding values of best-fit parameters. The initial parameter values are chosen randomly within reasonable intervals. For each replica, the goodness of the fit is evaluated using the usual χ^2 test, which corresponds to the error function of Eq. (A5), but with the original experimental data instead of the replicated ones.

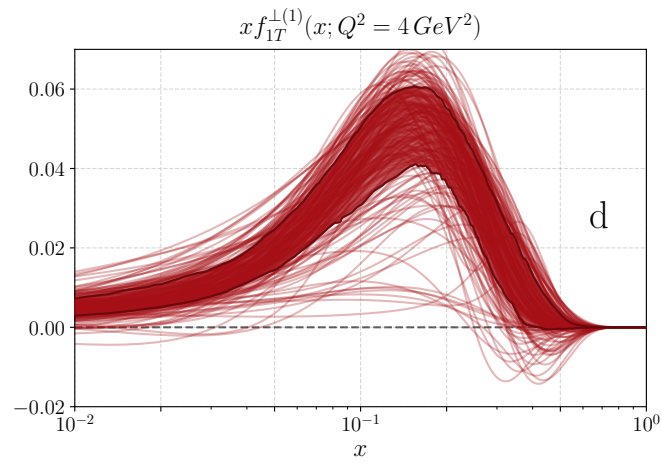
In Tab. I we give the value of the parameters obtained from our fit. For each one, we quote the central 68% of the 200 replica values (by quoting the average \pm the semi-difference of the upper and lower limits). Parameters of replica 105, used for the multidimensional plots, are also given.

	M_1	λ_S	α_d	α_u	α_s	
All replicas	0.97 ± 0.53	-0.47 ± 0.81	1.09 ± 0.96	0.22 ± 0.22	0.61 ± 0.54	
Replica 105	0.87	-0.85	2.01	0.14	0.27	
	β_d	β_u	β_s	A_d	A_u	A_s
All replicas	5.86 ± 4.13	2.00 ± 1.89	4.49 ± 4.45	-0.86 ± 21.70	-2.90 ± 4.26	3.08 ± 7.79
Replica 105	10.00	0.18	0.11	170.00	1.19	0.07
	B_d	B_u	B_s	N_{Siv}^d	N_{Siv}^u	N_{Siv}^s
All replicas	6.16 ± 12.30	2.24 ± 5.38	0.72 ± 3.50	$1.99 \times 10^{-6} \pm 1.00$	-0.09 ± 0.52	0.04 ± 0.54
Replica 105	87.60	2.49	0.35	-1.00	1.00	0.31

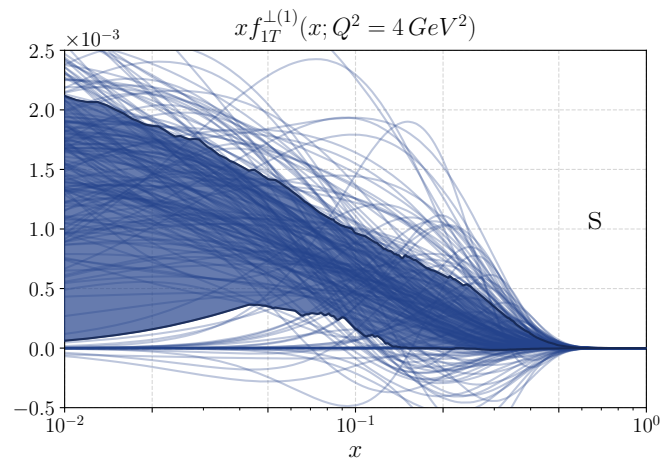
TABLE I. Values of best fit parameters for Siverson distribution. Upper rows contain the central 68% confidence intervals obtained by 200 replicas. Lower rows refers to the best fit parameters obtained from replica 105.



(a)



(b)



(c)

FIG. 3. The first transverse moment of the Sivers function, $x f_{1T}^{\perp(1)}$, as a function of x calculated for the up (a), down (b) and sea (c) quark at the scale $Q_0 = 1 \text{ GeV}$. The plots show all the 200 replicas obtained from the fit. For each value of x , the uncertainty bands contain the central 68% of the replicas.

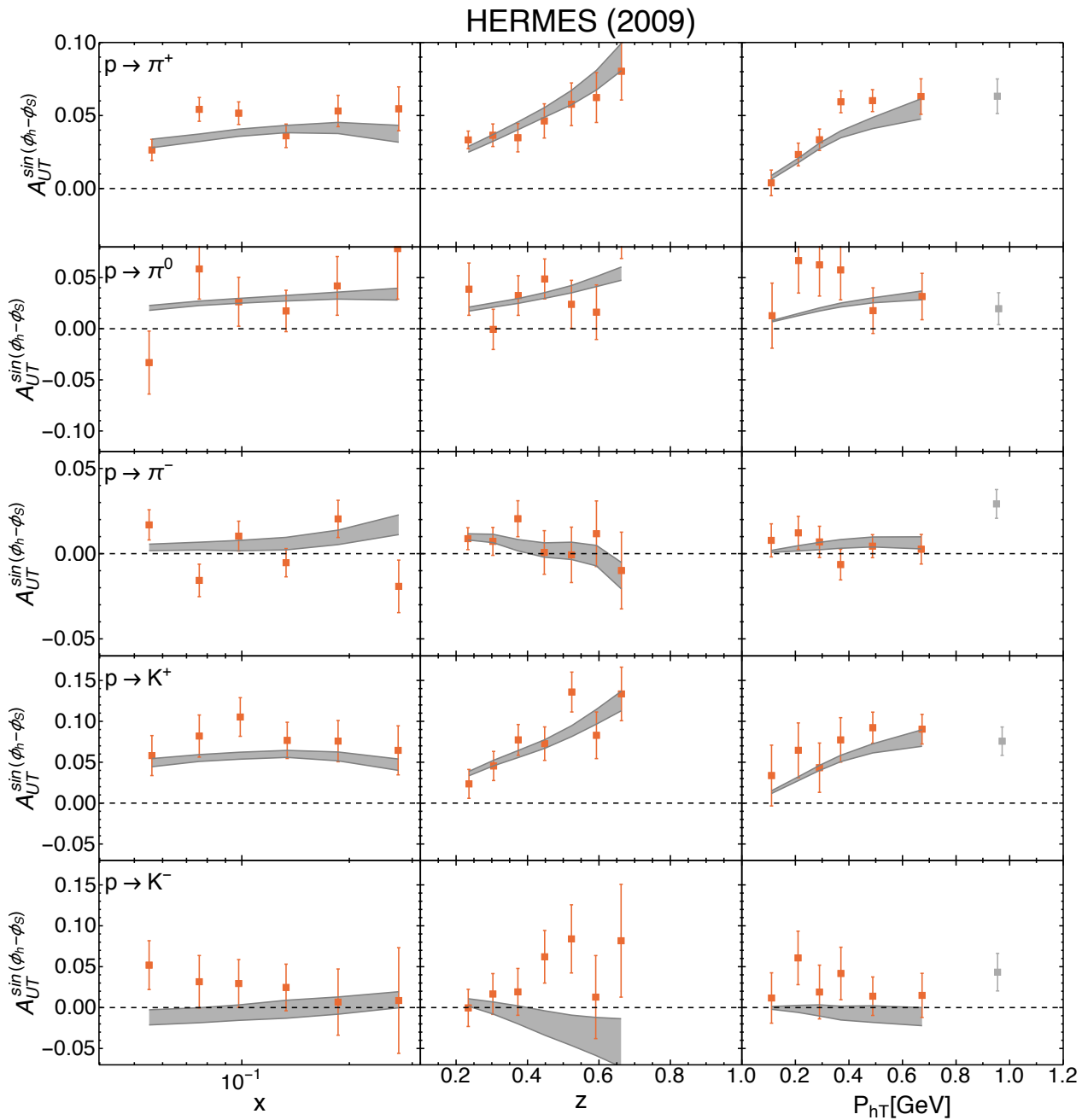


FIG. 4. HERMES Sivers asymmetries from SIDIS off a proton target (H) with production of π^+ , π^0 , π^- , K^+ , K^- in the final state, presented as a function of x , z , P_{hT} . Only the x -dependent projections have been included in the fit.

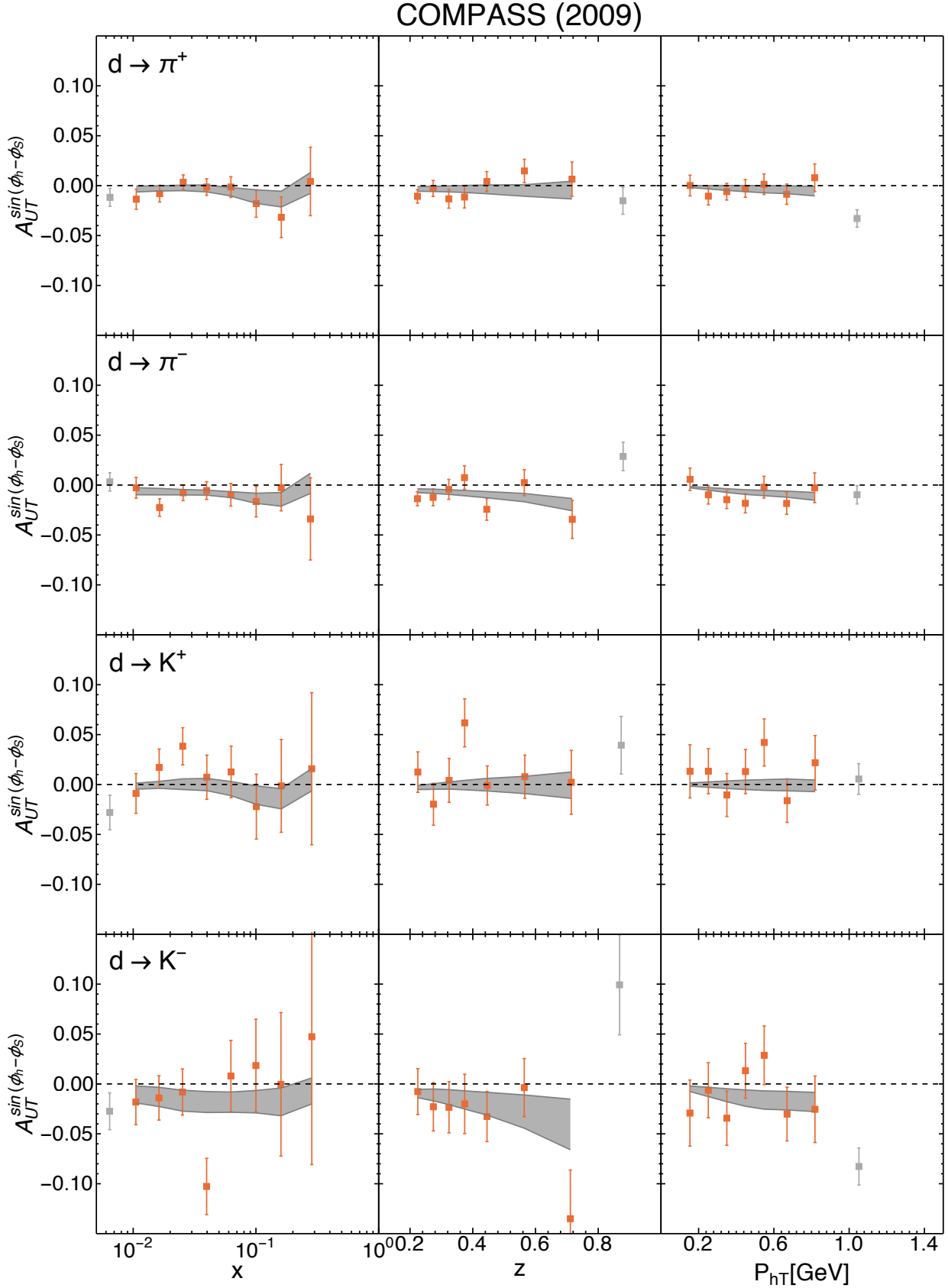


FIG. 5. COMPASS 2009 Sivers asymmetries from SIDIS off a deuteron target (${}^6\text{LiD}$) with production of π^+ , π^- , K^+ , K^- in the final state, presented as function of x , z , P_{hT} . Only the x -dependent projections have been included in the fit.

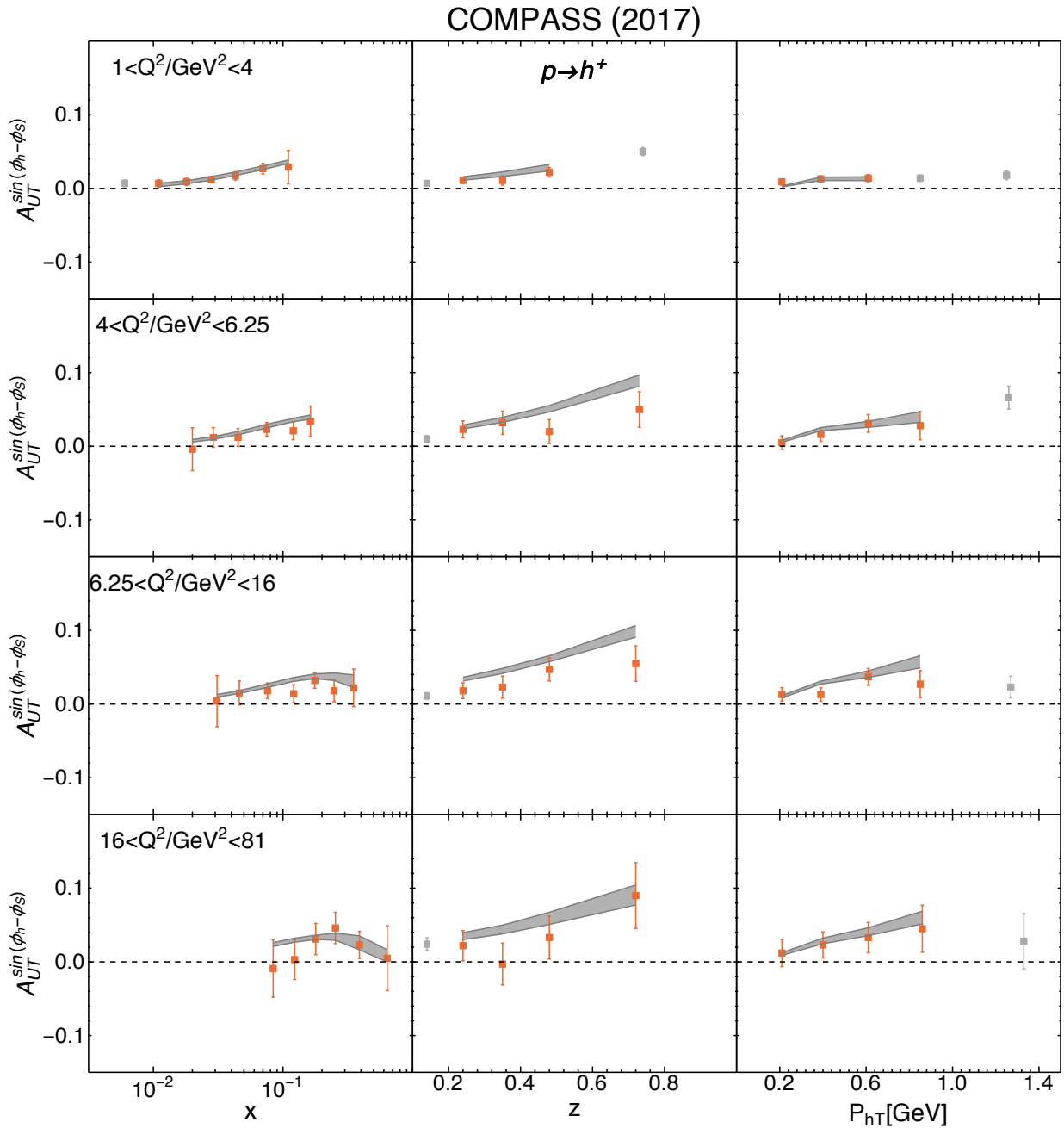


FIG. 6. COMPASS 2017 Sivers asymmetries from SIDIS off a proton target (NH_3) with production of positive hadrons h^+ , presented as function of x , z , P_{hT} and divided in four different Q^2 bins. Only the x -dependent projections have been included in the fit.

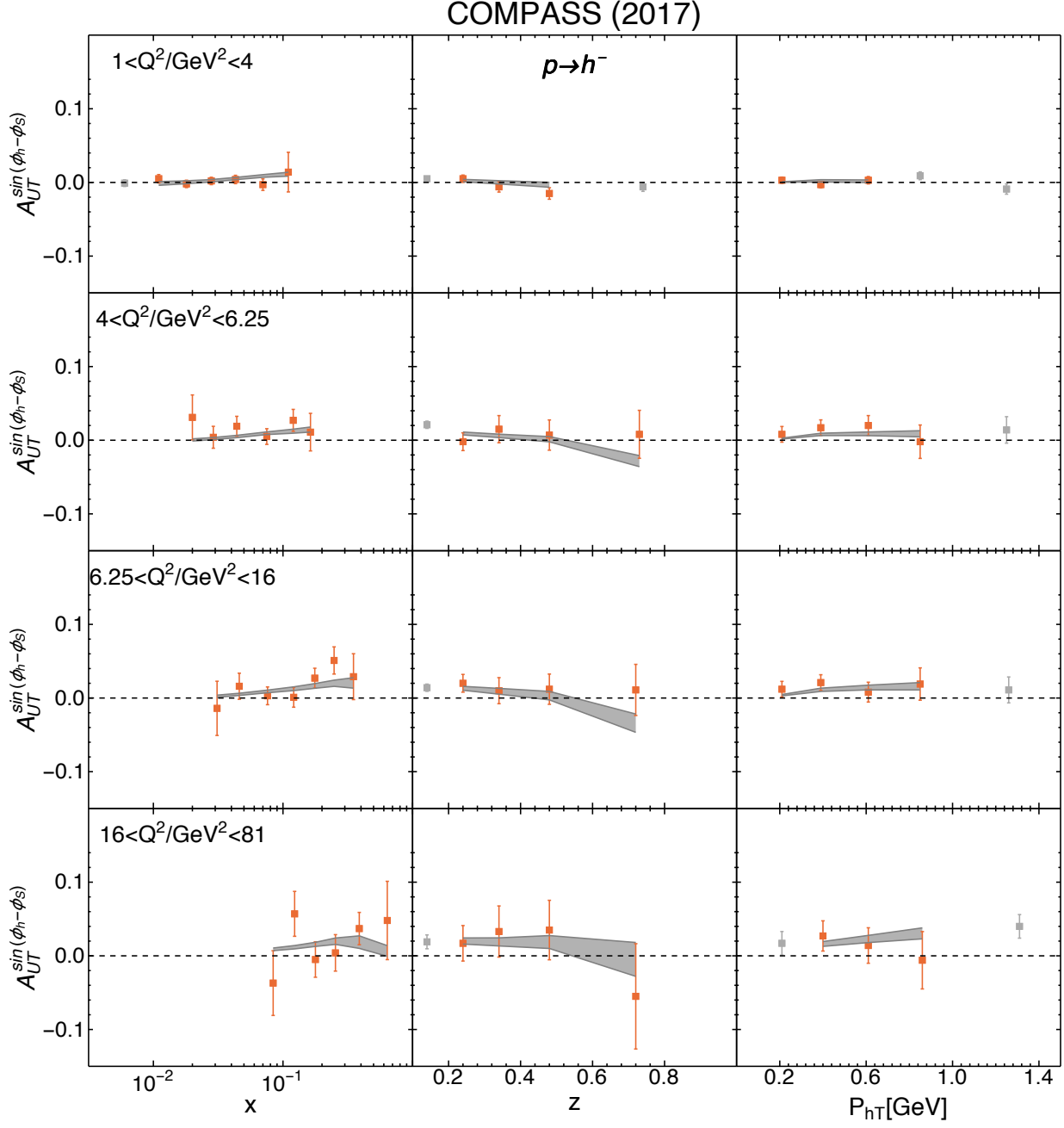


FIG. 7. COMPASS 2017 Sivers asymmetries from SIDIS off a proton target (NH_3) with production of negative hadrons h^- , presented as function of x , z , P_{hT} and divided in four different Q^2 bins. Only the x -dependent projections have been included in the fit.

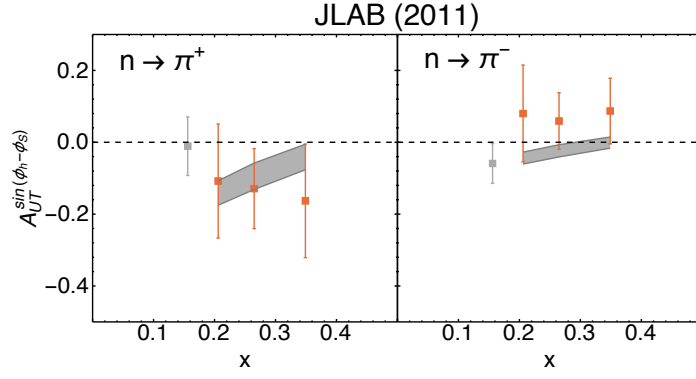


FIG. 8. JLab Sivers asymmetries from SIDIS off a deuteron target (${}^6\text{LiD}$) with production of positive and negative π in the final state, presented as function of x . Only the x -dependent projections have been included in the fit.